Sub-nanosecond, megawatt compact diode-pumped Nd:YLF laser

R.S. Cudney and C.E. Minor
Department of Optics, Centro de Investigación Científica y de Educación Superior de Ensenada, Carretera Ensenada-Tijuana 3918, Zona Playitas, 22860, Ensenada, B.C. Mexico.
e-mail: rcudney@cicese.mx

Received 2 April 2018; accepted 24 May 2018

We present a compact source of sub-nanosecond infrared laser pulses. The system is a diode-pumped, passively Q-switched Nd:YLF laser that emits 1.047 μm pulses with a FWHM duration of 750 ps, an energy of 2.3 mJ per pulse at a repetition rate of over 40 Hz. We also provide a simple rate-equation model that adequately describes the experimental results. This laser is ideal for several applications that require energetic sub-nanosecond pulses that cannot be obtained easily with actively Q-switched lasers or mode-locked lasers.

Keywords: Lasers; Q-switching; diode-pumped lasers.

PACS: 42.55.-f; 42.60.Gd; 42.55.Xi

1. Introduction

Many applications require simple and compact sources of pulses that are energetic (above 1 mJ), polarized and with pulsewidths between 50 ps and 1 ns, such as fluorescence lifetime decay spectroscopy [1], optical parametric generation and amplification of sub-nanosecond pulses [2], nonlinear frequency conversion to ultraviolet for Raman spectroscopy [3], among others. It is relatively easy to obtain 50 ps pulses with mode-locked lasers; however, the energy per pulse is low unless the pulses are amplified, which makes the system bulky, complicated and expensive. Actively Q-switched lasers can easily emit pulses orders of magnitude above 1 mJ, but since active Q-switches - mainly electro-optic and acousto-optic modulators - are big the cavity is long, which lengthens the round-trip time of the pulse in the cavity which in turn lengthens the pulsewidth; due to this, actively Q-switched lasers typically emit pulses longer than 5 ns.

The pulsewidth can be reduced by using passive Q-switching with saturable absorbers like Cr:YAG or semiconductor saturable-absorber mirrors (SESAM). There are reports where SESAM and micro-chips of Nd:YVO_4 have been used to obtain Q-switched pulses of 50 ps at a 40 kHz repetition rate with 1 μJ per pulse [4]; this approach has the potential to compete with amplified mode-locked lasers. Composite ceramics like Yb:YAG/Cr^{4+}:YAG have a larger damage threshold and have been used to produce 250 ps, 172 μJ pulses at a 3.5 kHz repetition rate [5]. Recently, a source of sub-nanosecond, megawatt ultraviolet pulses obtained from the fourth harmonic of a passively Q-switched Nd:YAG laser was reported [6].

Different materials doped with neodymium ions have been used as gain media. The material in which the ions are embedded affects the emission wavelength, lifetime of the upper state, and emission cross-section of the laser transition as well as the polarization of the emission. Nd:YLF is a uniaxial crystal that can be used to obtain strong, polarized laser lines, the strongest being in the 1.05 μm region, 1.047 μm for π polarization (polarization parallel to the crystal's c-axis) and 1.053 μm for σ polarization (polarization perpendicular to the crystal's c-axis); the 1.047 μm line has the largest stimulated emission cross-section. An advantage that this crystal has is that the lifetime of the upper state of the laser transition is large compared to that of more commonly used media, such as Nd:YAG and Nd:YVO_4. This allows more energy to be stored in the population inversion before it is dissipated by decay of the upper level, as explained in detail below, which translates into higher energy per pulse when it is used in a Q-switched laser. A disadvantage of this medium is that it is more susceptible to thermal load fracture than the other media mentioned above [7]. An appropriate design of the cooling system and the cavity is required to avoid damaging this crystal.

We present a compact source that emits pulses with a FWHM duration of 750 ps of more than 2 mJ. It is a diode-pumped laser that uses Nd:YLF as the gain medium and a saturable absorber, Cr:YAG, as the passive Q-switch. We also give a simple model that was used in the design of this laser and which gives results that predict fairly well the experimental results. The motivation for this work was to obtain a simple source to be used in our laboratory as a pump for mirrorless optical parametric oscillators [8], for time-resolved fluorescence spectroscopy [9], and for experiments in light-induced poling of ferroelectric materials [10,11].

2. Numerical model

We assume that the Nd:YLF crystal is pumped longitudinally with a collimated beam with a top-hat intensity distribution (constant intensity in a circle of radius w), but whose intensity decays with the direction of propagation z due to absorption, as shown in Fig. 1a). The transitions between the different levels of the Nd:YLF medium can be described by a simple four-level model, like the one shown in Fig. 1b). The medium is optically pumped from levels $|0\rangle$ to $|3\rangle$, from which the population rapidly decays to level $|2\rangle$. The lifetime

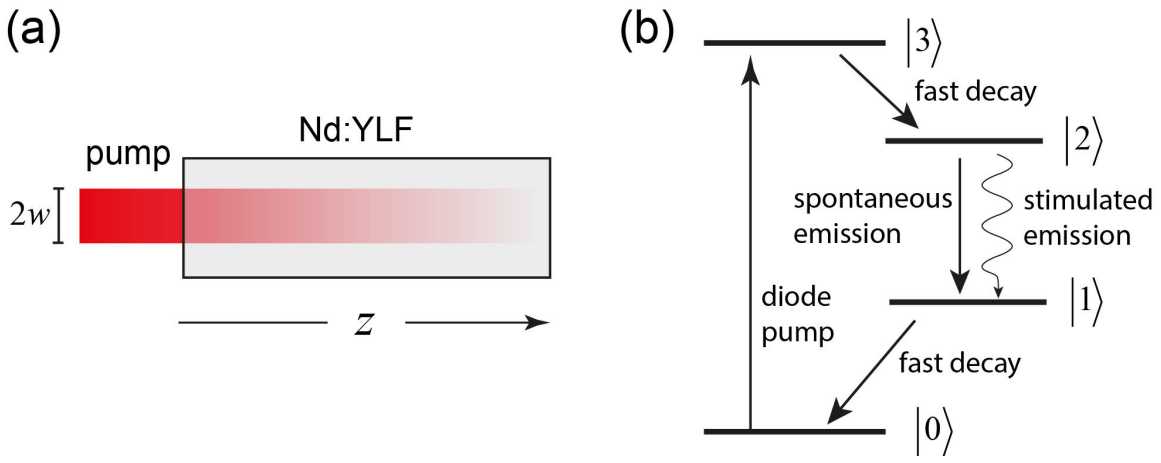

FIGURE 1. Pumping and transitions allowed in the model. a) Longitudinal pumping; b) four-level system.

of this level is assumed to be much longer than the lifetimes of levels $|1\rangle$ and $|3\rangle$; under this approximation the density N_1 of Nd ions in level $|1\rangle$ is negligible compared to the density N_2 of ions in level $|2\rangle$, so that the population inversion $\Delta N = N_2 - N_1 \approx N_2$. In the rate equation approximation, the time evolution of N_2 can be shown to be given by [12]

$$\frac{\partial}{\partial t}N_2(t,z) \approx \frac{\sigma_p \lambda_p N_T}{\pi w^2 hc} P_p(t,z) - \frac{N_2(t,z)}{\tau_2} - \frac{N_2(t,z)\Phi(t)\sigma_L c}{\pi w^2 L}. \quad (1)$$

The first term of the right-hand side of (1) represents the pumping of Nd ions to the level $|2\rangle$, while the second and third terms represent the spontaneous and stimulated decays of this level. Here h is Planck's constant, c is the speed of light, λ_p is the pump wavelength, N_T is the total density of Nd ions, τ_2 is the lifetime of level $|2\rangle$, Φ is the number of photons in the cavity, σ_p is the absorption cross-section of the pump beam, σ_L is the stimulated emission cross-section of the laser emission, L is the optical path length of the cavity, and w is the radius of the pump beam, which we assume for simplicity is constant throughout the entire cavity. P_p is the power of the pump beam; for longitudinal pumping this power decreases with the propagation distance by $P_p(z) = P_p(0)\exp[-\sigma_p N_T z]$, which also makes the population inversion dependent on z. We take this into account by using instead the spatial average $\langle N_2(t,z)\rangle$ of the population inversion, which in turn depends on the spatial average of the pump power $\langle P_p\rangle$, given by

$$\langle P_p\rangle = \frac{\int_0^d P_p(z)dz}{d} = \frac{\int_0^d P_p(0)\exp[-\sigma_p N_T z]dz}{d} = \frac{P_p(0)}{d\sigma_p N_T} f. \quad (2)$$

Here $f = 1 - \exp(-\sigma_p N_T d)$ is the fraction of the incident pump beam that was absorbed by the crystal and d is its length. Substituting (2) in (1), we get

$$\frac{\partial}{\partial t}\langle N_2\rangle \approx \frac{\lambda_p f}{d\pi w^2 hc} P_p(0) - \frac{\langle N_2\rangle}{\tau_2} - \frac{\langle N_2\rangle \Phi(t)\sigma_L c}{\pi w^2 L}. \quad (3)$$

The time evolution of the number of photons in the cavity is given by

$$\frac{d\Phi}{dt} = -\frac{\Phi}{\tau_c} + B\frac{\langle N_2\rangle}{\tau_2} + \langle N_2\rangle \Phi \sigma_L c\frac{d}{L} - N_{\text{base}}\Phi\sigma_{\text{base}}c\frac{d_{\text{abs}}}{L} - N_{\text{ex}}\Phi\sigma_{\text{ex}}c\frac{d_{\text{abs}}}{L}. \quad (4)$$

The first term of the right-hand side of (4) corresponds to the loss of photons due to the cavity, where the photon lifetime τ_c is given by

$$\tau_c = \frac{2L}{c(1 - R_i R_c e^{-2\alpha d})}, \quad (5)$$

where R_i and R_c are the reflectivities of the input mirror and the output coupler, respectively, and α are the passive losses of the gain medium. The second term is the spontaneous emission where B is a factor that takes into account that only a small fraction of these photons are emitted into the solid angle that corresponds to the cavity mode. The exact value of this parameter is not important (we set it to 10^{-4}); it is only required to seed the light amplification process. The third term represents the gain of photons due to stimulated emission, and the fourth and fifth terms are the photon losses due to absorption by the saturable absorber. We assume that the saturable absorber can be modeled as a two-level system [13], where N_{base} and N_{ex} are the density of Cr ions in the base and excited states, and σ_{base} and σ_{ex} are their cross-sections. The total number of Cr ions is given by $N_{\text{abs}} = N_{\text{base}} + N_{\text{ex}}$. We have assumed that the radius of the mode of the cavity matches the radius of the pump mode.

Finally, we need an equation for the time evolution of the Cr ions in the saturable absorber. This is given by

$$\frac{d}{dt}N_{\text{base}} = \frac{N_{\text{abs}} - N_{\text{base}}}{\tau_{\text{abs}}} - \frac{N_{\text{base}}\Phi\sigma_{\text{base}}c}{\pi w^2 L}, \qquad (6)$$

where τ_{abs} is the decay time of the excited state of the Cr ions. Normally the manufacturer of the Cr:YAG crystals does not specify the density and length of the crystal; instead, what is specified is its initial transmittance, which is given by

$$T_i = \exp[-\sigma_{\text{base}}N_{\text{abs}}d_{\text{abs}}], \qquad (7)$$

from which we can deduce that $N_{\text{abs}}d_{\text{abs}} = -\ln[T_i]/\sigma_{\text{base}}$. This is all the information we need since in (4) the densities N_{abs} and N_{ex} always appear multiplied by the saturable absorber thickness d_{abs}.

The instantaneous output power can be obtained from the number of photons in the cavity and is given by [12]

$$P_{\text{out}} = \frac{hc^2(1-R_c)}{2L\lambda}\Phi. \qquad (8)$$

The population inversion as a function of time when lasing is inhibited (below threshold) can be obtained by setting the number of photons $\Phi = 0$ and integrating (3) respect to time; we obtain

$$\langle N_2(z,t)\rangle = N_\infty(1-\exp[-t/\tau_2]), \qquad (9)$$

where $N_\infty = P_p(0)\lambda_p f\tau_2/d\pi w^2 hc$. The maximum population inversion that can be obtained is proportional to the upper state lifetime τ_2, which is why more energy can be stored in Nd:YLF, which has a lifetime of 520 μs, than in other media such as Nd:YAG and Nd:YVO_4 which have lifetimes of 230 and 90 μs, respectively.

We numerically solve Eqs. (3), (4) and (6) using the parameters given in Table I. We assume that the system is pumped with a rectangular pulse with a duration long enough to produce only one pulse from the laser, but never longer than $\tau_p = 2$ ms, which is almost 4 times the upper state lifetime τ_2. According to (9), for $\tau_p = 4\tau_2$ the population inversion is over 98% of the maximum; a longer pump pulse

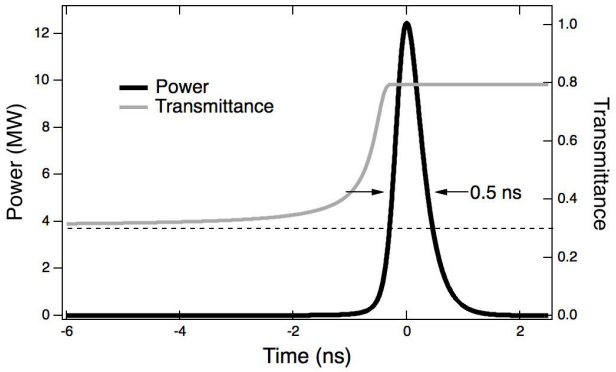

FIGURE 2. Pulse and Cr:YAG transmittance vs. time. Initial transmittance: 30%. Output coupler reflectivity: 50%.

TABLE I. Material and cavity parameters used in the simulations.

Parameter	Value
λ_p	798 nm
λ_L	1047 nm
τ_2	520 μs
N_T	6.9×10^{25} m^3
σ_p	5×10^{-24} m^2
σ_L	1.8×10^{-23} m^2
n_{YLF}	1.470
d	12 mm
σ_{base}	4.3×10^{-22} m^2
σ_{ex}	8.2×10^{-23} m^2
τ_{abs}	3.4 μs
w	500 μm
L	28 mm
α	0.1 cm^{-1}

is pointless since the decay of the upper level limits the population inversion that can be achieved. The cavity optical path length $L = 29$ mm and pump radius $w = 500$ μm given in the table correspond to the values used in our experimental set-up. We assume that the pump beam, which is delivered by a multimode fiber, is depolarized and is tuned to the absorption peak of Nd:YLF that occurs at 797-798 nm. Under these conditions, for a 12 mm long crystal with 0.5% Nd ion concentration, more than 98% of the pump should be absorbed. Figure 2 shows an example of the pulses obtained with the simulations. Here the initial transmittance is 30%, pump power 50 W, and output coupler reflectivity 50%. As can be seen, the FWHM pulse duration is 0.5 ns and the peak power is over 10 MW, which is suitable for the applications mentioned above. The variation in time of the transmittance of the Cr:YAG crystal is also shown. It changes dramatically from slightly above 0.3 to 0.8 in about two nanoseconds; complete bleaching is achieved less than a nanosecond before the peak of the pulse occurs.

Figure 3 shows the pulsewidth and energy per pulse vs. pump power for a fixed value of the output coupler reflectivity (50%) and for different values of the initial transmittance of the saturable absorber (30, 50, 70 and 90%). Again, the crystal is pumped with a 1.9 ms rectangular pulse. From these simulations we see that the minimum power required to obtain a pulse increases as the initial transmittance decreases. After this threshold is met, neither the pulsewidth nor the energy per pulse change significantly with pump power. This is to be expected. The saturable absorber requires a certain amount of fluence in order to be bleached, and this fluence increases with decreasing initial transmittance. Once the saturable absorber is bleached, most of the remaining energy stored as a population inversion in the gain medium is extracted by the pulse. Pumping above this threshold only reduces the time that the laser pulse occurs within the pump pulse, but does not increase its energy.

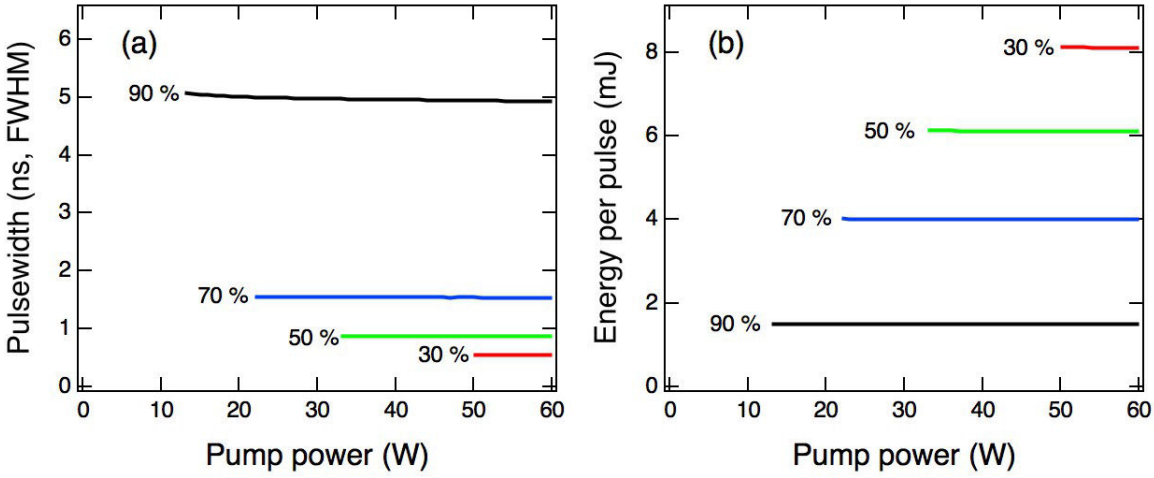

FIGURE 3. Numerical results: Dependence with pump power. a) Pulsewidth; b) energy per pulse. The percentages shown are the values of the initial transmittance of the saturable absorber. Output coupler reflectivity: 50%.

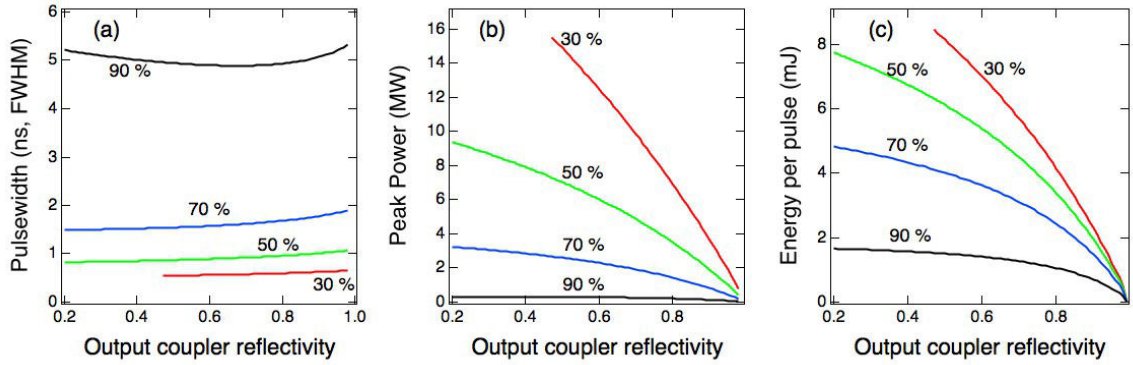

FIGURE 4. Numerical results: Dependence with output coupler reflectivity. a) Pulsewidth; b) peak power; c) energy. The percentages shown are the values of the initial transmittance of the saturable absorber. Pump power: 50 W.

Figure 4 shows the results of the simulations when the output coupler reflectivity is varied, assuming $P_p = 50$ W of which 98.5% is absorbed. Figure 4 a) shows the FWHM pulsewidth vs. output coupler reflectivity for a few Cr:YAG saturable absorbers with different initial transmittances. The pulse width does not depend strongly on the reflectivity of the output coupler but does depend strongly on the initial transmittance. Figure 4 b) and c) show the peak power and energy per pulse vs. output coupler reflectivity. In these cases, both the output coupler reflectivity and the initial transmittance affect the output energy. From these simulations we see that in principle we can obtain sub-nanosecond pulses of more than 8 mJ if a 30% initial transmittance saturable absorber is used.

3. Experiment

The basic set-up used for our experiments is shown in Fig. 5. As a pump source we used a pulsed diode laser coupled to a 600 μm in diameter core, NA = 0.22 fiber. The output of the fiber was collimated by a 6 mm focal length lens and then focused onto a 12 mm long, a-cut Nd:YLF crystal. We used several Cr:YAG crystals as saturable absorbers with different initial transmittances. In order to avoid their fracture due to thermal stress, both the Nd:YLF and the Cr:YAG were covered with indium foil and placed inside a metal block to extract the heat produced by the pump. The temperature of the block was regulated by a Peltier cooler and kept at 18°C. The input mirror was flat, highly reflecting (> 99 %) at 1.047 μm

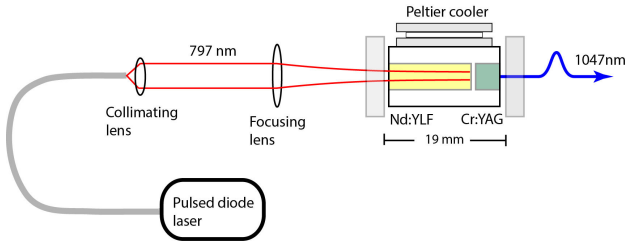

FIGURE 5. Experimental set-up. Fiber: 600 μm in diameter core, NA=0.22; collimating lens: 6 mm focal length. Several focusing lenses with different focal lengths were used.

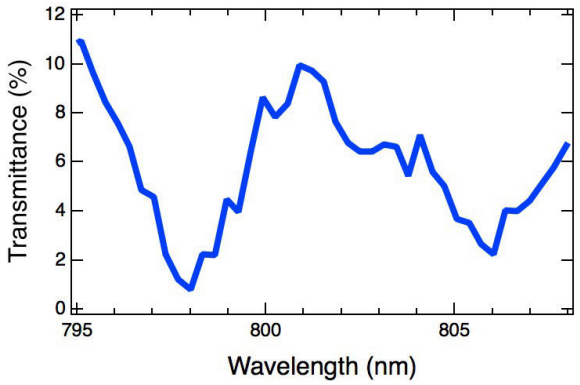

FIGURE 6. Transmittance of Nd:YLF vs. wavelength.

and highly transmitting ($> 95\%$) at the pump wavelength, 798 nm. We used several output couplers with different reflectivities and different radii of curvature, ranging from flat to 500 mm. In order to reduce the pulsewidth, the cavity was made as short as possible, limited by the size of the components, 19 mm.

In order to maximize the fraction of the pump absorbed by the Nd:YLF crystal and at the same time minimize the pump power incident on the Cr:YAG, which would cause undesired partial bleaching and heating, we must pump with a wavelength that coincides with an absorption peak. Figure 6 shows the transmission of Nd:YLF as a function of wavelength for depolarized light. In the region shown in this figure, the highest absorption occurs at 798 nm. We adjusted the temperature of the diode to achieve this wavelength, obtaining emission centered at 798 with a FWHM bandwidth of 2.5 nm. According to the supplier of our crystal (Red Optronics), the Nd concentration is 1%, not the 0.5% used in our calculations. However, the fraction f of the pump that is absorbed by the gain medium, which ultimately is the parameter that matters, is approximately 0.985, which is the factor used in the numerical analysis. The discrepancy most likely is due to a few factors, such as the bandwidth of the pump, inaccuracies of the absorption cross-section of the medium and partial polarization of the pump beam.

Several arrangements with different output couplers and Cr:YAG crystals were tested and measured. In all cases the trend agreed with the numerical predictions: the lower the initial transmittance of the Cr:YAG, the shorter the pulse, and the lower the reflectivity of the mirror, the more energetic the pulses as well as the more pump power required to obtain them. Examples of the measurements of the pulsewidth and energy per pulse for five different values of the initial trans- mittance of the saturable absorber are shown in Fig. 7. In all five cases the output coupler, cavity length, pump beam width, and repetition rate were the same; only the initial transmittance and the pump power required to obtain the pulses were changed for each data point.

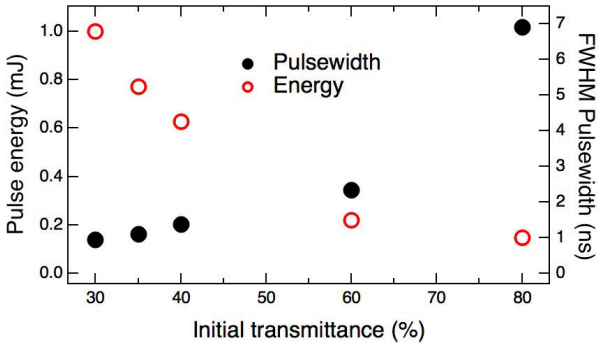

FIGURE 7. Pulsewidth and energy per pulse vs. initial transmittance.

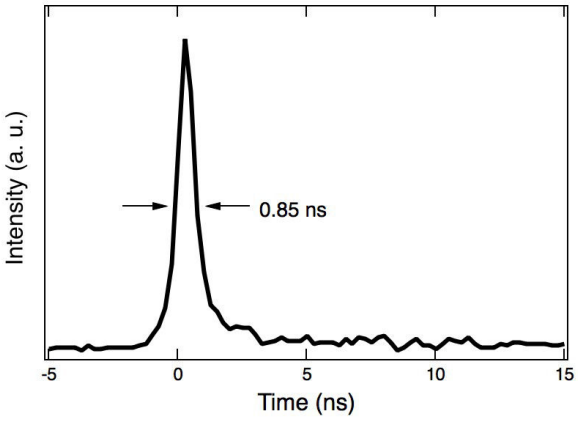

FIGURE 8. Q-switched pulse.

Since our goal was to make a Q-switched laser with the shortest pulsewidth possible, we concentrated our efforts on the configuration where the shortest and most energetic pulses were obtained. This was accomplished with a Cr:YAG with a 30% initial transmittance and a flat output coupler with 55% reflectivity. The total optical path length taking into consideration the refractive indices of both crystals was 29 mm. The focal length of the focusing lens was 60 mm and the resulting width of the pump beam at the input surface of the Nd:YLF crystal was $w \approx 500$ μm. The minimum pump power required to obtain Q-switched pulses was 50 W, with a pump pulse duration of 1.9 ms. Figure 8 shows an example of the pulses obtained with this configuration, measured with a 1 GHz, 4 gigasamples/sec oscilloscope and a InGaAs PIN detector with a 175 ps rise time. According to the oscilloscope trace, the pulsewidth is 850 ps; however, this trace is the result of the convolution of the real pulse and the response of the detecting system (oscilloscope and detector), which cannot be neglected. The measured pulsewidth is given by [14]

$$\tau_{\text{measured}} \approx \sqrt{\tau_{\text{real}}^2 + \tau_{\text{osc}}^2 + \tau_{\text{det}}^2}, \tag{10}$$

where τ_{measured} and τ_{real} are the measured and real pulsewidths, respectively, and τ_{osc} and τ_{det} are the response times of the oscilloscope and the detector. The response time of the oscilloscope is $\tau_{\text{osc}} \approx 0.35/\text{bandwidth} = 350$ ps. From (10) we conclude that the real pulsewidth $\tau_{\text{real}} \approx 750$ ps.

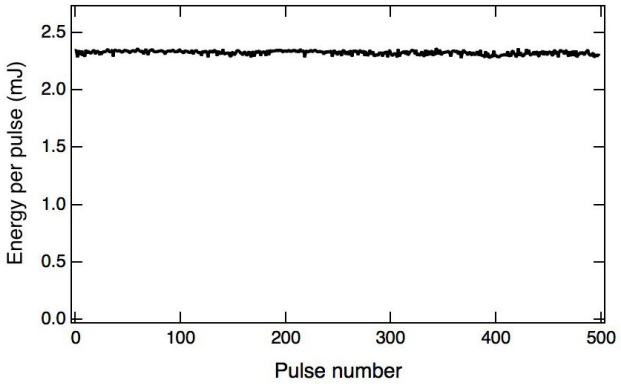

FIGURE 9. Pulse energy vs. pulse number. Repetition rate: 40 Hz. Pump power: 50 W. Pump pulsewidth: 1.9 ms.

Figure 9 shows the energy per pulse vs. pulse number when the laser is pumped at a 40 Hz repetition rate. The system is very stable; the energy per pulse averaged over the 500 pulses shown in Fig. 9 is 2.32 mJ with a standard deviation of only 0.018 mJ. The peak power of these pulses is over 3 MW. Neither the energy per pulse nor the pulsewidth depend on the pump power, provided it is above the threshold required to obtain a pulse, which agrees with our simulations.

We also estimated the bandwidth of the pulses and their spatial quality. To estimate the bandwidth we sent the pulses through a Michelson interferometer and observed the visibility of the interference pattern as a function of the path length difference. We found that the visibility of the fringes decreases significantly for path length differences above approximately 12 cm, corresponding to a time delay of ~ 400 ps, around half the pulsewidth. From this we conclude that the spectrum of the pulse is close to the Fourier limit; in other words, it emits in a single-longitudinal or almost single-longitudinal mode. As for the spatial quality, in the vertical direction (along the crystal's c axis) we obtained $M_y^2 = 3.5 \pm 0.2$ and $M_x^2 = 2.9 \pm 0.1$ in the horizontal direction. This is actually very good, considering that the cavity consists of two plane mirrors, which is borderline unstable, and matching of the pump and cavity modes was not performed.

Finally, as an example of its use in intended applications, we used this laser to obtain cascaded nonlinear processes in a single aperiodically poled lithium niobate crystal (APPLN). Using the procedure outlined in [15], the APPLN crystal was designed to simultaneously produce optical parametric generation (1.047 μm $\rightarrow$ 1.46 μm + 3.69 μm) and sum-frequency generation between the pump and the signal produced by the optical generation process (1.047 μm + 1.46 μm $\rightarrow$ 610 nm). The electrical poling technique as well as the procedure to make the mask required to create the poling electrodes are described in detail in [16]. The dimensions of the APPLN crystal were $20 \times 20 \times 0.5$ mm. Figure 10 shows the experimental set-up used to generate and detect the pulses at 610 nm produced with our laser and our APPLN crystal. The energy per pulse incident on the APPLN crystal was controlled

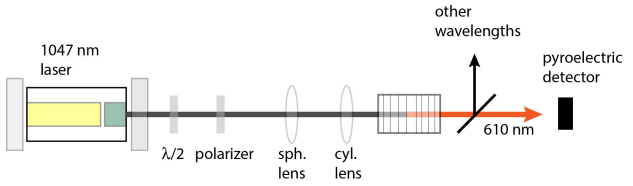

FIGURE 10. Experimental set-up for the generation and detection of short pulses of 610 nm through cascaded nonlinear interactions in APPLN.

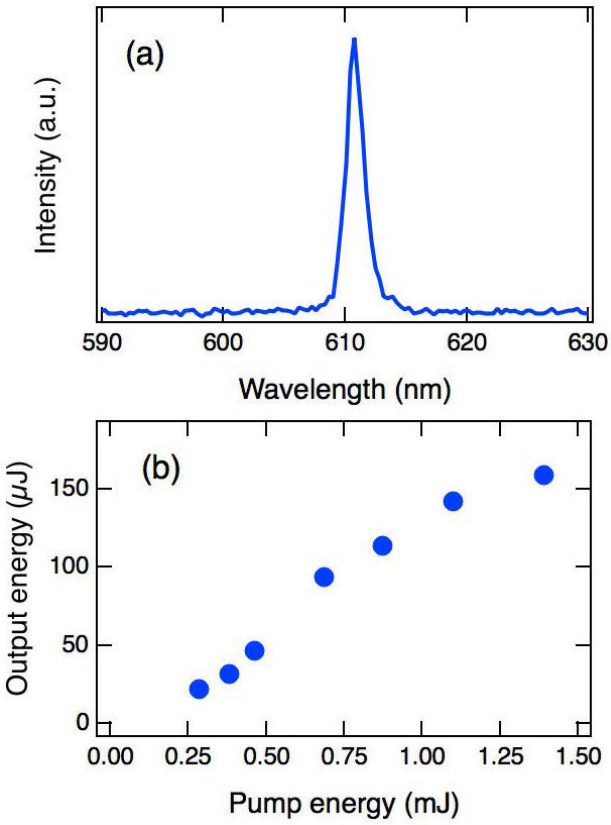

FIGURE 11. Generation of 610 nm pulses through cascaded nonlinear interactions. a) spectrum of the pulses; b) 610 nm pulse energy vs. pump energy.

by a half-waveplate and a Glan-Thompson polarizer. Since the APPLN crystal is only 500 μm thick, it was necessary to use a pump with an elliptical cross-section to be able to send the entire beam through the crystal without exceeding the damage threshold fluence, which is around 2 J/cm^2 for pulses that have a duration of the order of 1 ns. This was accomplished by sending the pulses through a combination of a spherical lens ($f = 175$ mm) and a cylindrical lens ($f = 150$ mm), with which we obtained an oval-shaped beam of approximately 0.25×1 mm, FWHM, which has an area of $\approx 2 \times 10^{-3}$ cm^2. Even when the total energy per pulse was used (≈ 2.2 mJ) the fluence was ~ 1 J/cm^2, which is lower than the crystal's damage threshold. The remnant pump pulse as well as the optical parametric generation signal and idler pulses were removed using dichroic filters and the remaining

610 nm pulses were detected by a well-calibrated pyroelectric detector.

The results are shown in Fig. 11. Figure 11a) shows the measured spectrum; we obtained a pulse at 610.7 nm, very close to the 610 nm design wavelength. Figure 11b) shows the energy of the 610 nm pulses vs. the pump energy. We obtained a conversion of over 11%, which is high considering that the pulses were produced with two cascaded nonlinear interactions in a single-pass through the crystal. Enclosure of the APPLN crystal in a two-mirror cavity to obtain feedback (optical parametric oscillation) was not required due to the high peak intensity of the 750 ps pump pulses.

4. Conclusions and final remarks

We presented a diode-pumped, compact passively Q-switched laser that can emit pulses with pulsewidths lower than 1 nanosecond, more than 2.3 mJ per pulse and peak powers above 3 MW. The high energy and small pulsewidth are due in part to the use of Nd:YLF as the gain medium, since its upper state's lifetime is large, which allows more energy to be stored in the crystal. By using Cr:YAG saturable absorbers with different initial transmittance values we could vary the pulsewidth from 6.8 ns to 750 ps.

We also presented a simple model that predicts fairly well the pulsewidth and the pump power required to obtain the pulses as a function of the cavity length, output coupler reflectivity and initial transmittance of the saturable absorber. The energy per pulse that we measured follows the trend predicted by the model: the lower the initial transmittance the higher the energy per pulse and the higher the pump power required; however, the measured energy is more than 3 times less than what is predicted. Most likely this is due to one of the assumptions in the model, namely, that the pump mode and cavity mode overlap perfectly in a cylinder of radius w, which is a simplification that may be far from valid. By carefully designing the cavity in order to match the pump and cavity modes, taking into account thermal lensing of gain medium, the energy per pulse could increase; however, this is beyond the scope of this work.

Finally, as an example of its intended applications we used this laser to produce cascaded nonlinear interactions in an aperiodically poled lithium niobate crystal, obtaining short pulses of more than 150 μJ at 610 nm.

Acknowledgments

The authors thank D. Yankelevich for many discussions and encouragement, and L.A. Rios for assistance on technical issues. C.E. Minor gratefully thanks Bruno Zedrick for motivating the development of this work. This research was partially funded by the Consejo Nacional de Ciencia y Tecnología (CONACYT), grant 2010-01- 156442, and by UC-Mexus, grant CN-17-135.

1. Y. Sun *et al*., *Rev. Sci. Instrum.* **80** (2009) 065104
2. H. Ishizuki and T. Taira, *Opt. Express* **24** (2016) 1046
3. M. A. Troyanova-Wood, G. I. Petrov and V. V. Yakovlev, *J. Raman Spectrosc.* **44** (2013) 1789
4. D. Nodop, J. Limpert, R. Hohmuth, W. Richter, M. Guina and A. Tünnermann, *Opt. Lett.* **32** (2007) 2115
5. J. Dong, K. Ueda, A. Shirakawa, H. Yagi, T. Yanagitani, and A. A. Kaminskii, *Opt. Express* **15** (2007) 14516
6. R. Bhandari and T. Taira, *Opt. Express* **19** (2011) 22510
7. E. H. Bernhardi, A. Forbes, C. Bollig and M. J. D. Esser, *Opt. Express* **16** (2008) 11115
8. C. E. Minor, R. S. Cudney, *Appl. Phys. B* **123** (2017) 38.
9. D. Ma, J. Bec, D. Yankelevich, D. Gorpas, H. Fatakdawala and L. Marcu, *J. Bio. Med. Opt.* **19** (2014) 66004
10. S. Mailis, *J. Opt.* **12** (2010) 095601
11. H. Steigerwald *et al.*, *Phys. Rev. B* **82** (2010) 214105
12. O. Svelto, *Principles of Lasers* (Springer, New York)
13. A. Sennaroglu, *et al.*, *J. Opt. Soc. Am. B* **23** (2006) 241
14. P. R. Bolton, *Lawrence Livermore National Laboratory Livermore Report UCID 21096*, (1987)
15. M. Robles-Agudo, R.S. Cudney, *Appl. Phys. B* **103** (2011) 99
16. R. S. Cudney, L.A. Ríos, M. J. Orozco Arellanes, F. Alonso, J. Fonseca, *Rev. Mex. Fis.* **48** (2002) 548